INFLUENCE OF COLD PLASTIC DEFORMATION ON THE SENSITIZATION OF AISI 304L STAINLESS STEEL AND SERVICEABLENESS OF EPR METHOD

T. Pastore, B. Mazza and A. Cigada
Dipartimento di Chimica Fisica Applicata, Centro di Studio del CNR sui Processi Elettrodici, Politecnico di Milano, Piazza Leonardo da Vinci 32, 20133 Milano, Italy

ABSTRACT — This work studies the influence of cold plastic deformation and the possible formation of martensite on the susceptibility to intergranular corrosion (I.G.C.) of austenitic stainless steels. The tests were made on an AISI 304 L steel, cold rolled to various reduction ratios and heat treated between 300 and 500 °C. Furthermore, the applicability of the electrochemical potentiokinetic reactivation (EPR) test to determine the susceptibility of cold plastic-deformed materials to I.G.C. was verified, also in view of a draft standard.

The effect of cold plastic deformation on stainless steel sensitization has been known for a long time. However, the relevant literature is rather limited when compared to that covering other aspects of intergranular corrosion susceptibility. The importance of cold plastic deformation on sensitization was recently brought to light since in practice all steels are somewhat deformed before, during or after heating to sensitizing temperatures. In any of these three cases, the susceptibility to intergranular corrosion may differ from that of undeformed steel (1-7).

The effect of cold plastic deformation, performed before or during the sensitizing treatment, can best be explained on the basis of the theory of chromium depletion, commonly accepted for undeformed steel. Cold plastic deformation induces structural changes within the austenitic matrix, which help diffusion processes and chiefly chromium diffusion. Room temperature deformation essentially causes dislocation density to increase and deformation bands to form and develop. Consequently, when degree of deformation increases, the chromium-rich carbides nucleate and grow more rapidly and carbide precipitation inside the grain may occur. At the same time, chromium rediffuses in those areas that have been depleted by carbide precipitation.

While the sensitization rate increases with the degree of deformation, healing too is more rapid. This is especially evident at higher temperatures when the maximum sensitizing temperature progressively drops, since the greater the deformation the easier the rediffusion of chromium. At lower temperatures, healing should however occur after much longer heating times, and only the acceleration effect on the sensitization process is of practical significance. Matrix deformation would therefore always have a harmful effect.

Besides the structural changes mentioned before, the deformation of an austenitic stainless steel, when sufficiently high in relationship to deformation temperature may cause α' - martensite to form. Its presence is not always considered although it too has a similar accelerating effect on the sensitization process due, among other things, to lower carbon solubility.

It is in order to remark that the different morphology of carbide precipitation in a highly deformed steel should induce corrosion behaviour characteristics that differ from those of a similarly sensitized, undeformed steel; furthermore, sensitization is no longer correlated to intergranular corrosion susceptibility. Therefore, the degree of sensitization, as measured by the current chemical or electrochemical tests, may be affected by their characteristics.

This work studies the influence of cold plastic deformation and of the possible formation of martensite on the susceptibility to intergranular corrosion (I.G.C.) of austenitic stainless steels. The tests were made on an AISI 304L steel, cold rolled to various reduction ratios and heat treated between 300 and 500°C. Furthermore, the applicability of the electrochemical potentiokinetic reactivation (EPR) test to determine the susceptibility of cold plastic-deformed materials to intergranular corrosion was verified.

EXPERIMENTAL

Bars having dimensions 250x25x15 mm were cut from a plate of AISI 304L steel, the composition of which is given in Table 1. The bars were

Table 1 - Chemical composition (wt%) of the AISI 304L stainless steel under study

C	N	Si	Mn	Cr	Ni	Mo	Cu	P	S
0.020	0.039	0.41	1.40	18.10	10.30	0.32	0.24	0.032	0.013

heat treated at 1050°C for one hour and successively water-quenched (solution annealing

Table 2 - Structural properties of AISI 304L stainless steel as a function of cold plastic deformation conditions

Type	Deformation Temperature (°C)	Deformation Degree* (%)	X-Ray diffraction Phases	Magnetic measurements Ferro-magnetic phase (wt%)	Transmission electron microscopy Dislocation density ($\times 10^9$ cm/cm^3)	Deformation bands	α'-Martensite	Austenite
Rolling		0	γ	0.05	1.0	-	-	≃ 100%
	25	10	γ +α'(v.l.)	0.14	17	m.q.	n.o.	l.p.
		30	γ +α'(v.l.)	0.60	>20	p.	n.o.	l.p.
		50	γ +α'(l.)	2.35	>20	p.	n.o.	l.p.
	-196	10	γ +α'(m.q.)+ε(v.l.)	26.2	-	m.	m.q.	p.
		30	γ +α'(p.) +ε(v.l.)	63.0	-	p.	v.m.	m.q.
		50	γ +α'(l.p.)+ε(v.l.)	86.5	-	h.d.	l.p.	n.d.

Notes: * Quantified as reduction in thickness. v.l. = very little (<1%); l. = little (1 ÷ 10%); m.q. = medium quantity (10 ÷ 40%); m. = much (40 ÷ 50%); v.m. = very much (50 ÷ 60%); p. = prevailing (60 ÷ 80%); l.p. = largely prevailing (>80%); n.o. = not observed; n.d. = not discernible; h.d. = hardly discernible; s.d. = still discernible.

treatment, SA) to remove the structural changes induced by the manufacturing process and to reinstate a homogeneous austenitic structure. Afterwards, some bars were cold rolled and their thickness reduced by 10%, 30% and 50% at room temperature (R.T.) and at liquid nitrogen temperature (-196°C), by the procedure described in earlier papers (8-10). These papers also give the characteristics of the steel after rolling and describe its behaviour towards other forms of corrosion.

The metallurgical conditions are summarized in Table 2. The room temperature rolled steel maintains the austenitic matrix of the solution-annealed material; only when thickness reduction is 50% a non negligible, but slight amount of α'-martensite forms. Rolling at liquid nitrogen temperature causes large amounts of martensite to form; as the deformation degree increases, this phase becomes predominant (Fig. 1). Therefore, the initial material is representative of two conditions: in the one, residual stress effects predominate and increase with the deformation degree; in the other, these effects are concurrent with that of martensite.

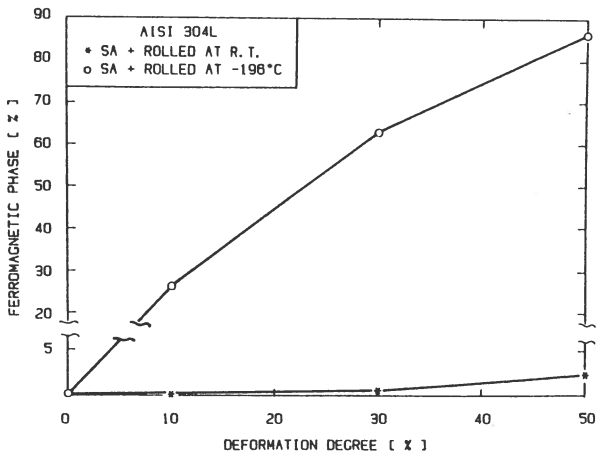

Figure 1 - Ferro-magnetic phase content (wt%) of AISI 304L stainless steel as a function of cold plastic deformation conditions

After cropping and discarding the bar ends, cylindrical testpieces having a height equal to half the bar thickness were cut from the bars. The testpieces were heat treated in nitrogen atmosphere at 300°C for 100 and 1000 h; at 400°C and 500°C for 1 h, 10 h, 100 h and 1000 h followed by water quenching. Oxalic acid etch tests, weight loss measurements during the modified Strauss test and EPR tests were executed. For each condition of the material, two specimens were tested on the rolling surface; the weight loss measurements were performed on the entire surface of the specimens. The testpieces were wet-ground with emery paper up to 1000 mesh for the weight loss test and further polished with diamond paste up to 3 μm for the oxalic acid test and to 1/4 μm for the EPR test. The polished testpieces were degreased in acetone, rinsed with distilled water and dipped in ethyl alcohol for 15 min in all.

The oxalic acid etch test was performed as specified in ASTM A 262 Practice A, to detect steel structure after thermo-mechanical treatment and to measure the austenitic grain size. This measurement was made according to the linear intercept method of the ASTM E 112 standard.

The $Cu/CuSO_4$ solution dipping tests were executed as specified in ASTM A 262 Practice E for the modified Strauss test. Susceptibility to intergranular corrosion was determined by weight loss measurement. The testpieces were periodically removed, rinsed in distilled water in the presence of ultrasonic vibrations, dried and weighed. Any copper buildup on the surface was removed by dipping in concentrated nitric acid. Six testpieces were dipped in the boiling test solution (800 ml) and placed in contact with the metallic copper but not in contact with each other. The test was made on non rolled steel (specimen surface area 5.19 cm^2), on steel rolled by 10% at room temperature (4.98 cm^2), and on steel rolled by 10% at -196°C (4.86 cm^2).

The EPR test was carried out as suggested by Clarke et al. (11), by the procedure described in former papers (12,13) and summarized in Table 3. The testpiece was left for 8 min in a deaerated 0.5 M H_2SO_4 + 0.01 M KSCN solution and the free corrosion potential E_{corr} read (this always ranged within -425 mV and -445 mV vs SCE; therefore, no cathodic activation was performed). The testpiece was then passivated at +200 mV vs SCE for 2 min and brought back to E_{corr} potential, scanning at 100 mV/min, to measure the circulated charge Q. The latter was then normalized with respect to the grain boundary area (GBA) (11). At the end of the test, the testpieces were examined under the optical and scanning electron microscopes and the surface area exposed to the testing environment was obtained by measuring two orthogonal diameters.

Table 3 - EPR test conditions

Solution	0.5 M H_2SO_4 + 0.01 M KSCN
Temperature	30 ± 1 °C
Deaeration	Nitrogen 9 l/h
Specimen surface area	0.66 cm^2
Specimen surface finish	1/4 µm diamond paste, 1 h before testing
Reference electrode	Saturated calomel electrode (SCE)
Free corrosion time	8 min
Cathodic activation	5 min at -600 mV only if corrosion potential is not between -350 and -450 mV
Passivation	2 min at +200 mV
Sweep rate and direction	6 V/h, cathodic

RESULTS AND DISCUSSION

Table 4 is a summary of the oxalic acid tests; Figs. 2-6 show the more significant microstructures observed.

The non-rolled steel always has a "step" structure (Fig. 2a), that is the typical microstructure of a steel without carbide precipitation at grain boundary. The only exceptions are the testpieces treated at 500°C for 1000 h, which exhibit intergranular carbide precipitation and a consequent "ditch" structure (Fig. 4a).

The steel rolled by 10% at room temperature, exhibits microstructures which vary with the heat treatment conditions in a similar way to that of non-rolled material; a ditch structure only occurs after treating at 500°C for 1000 h (Figs. 2b and 4b). Furthermore, rolling- induced deformation bands can be seen. These bands seem to affect carbide precipitation: indeed, besides evidencing intergranular carbides, Fig. 4b shows etching inside the grain (E.I.G.), possibly due to carbide precipitation on the deformation bands. In these areas, starting from the crossing of two deformation bands, intragranular carbide precipitation appears to precede the intergranular one and to occur after 1000 h at 400°C (Fig. 5). The greater the deformation degree, the larger the number of deformation bands; however, the structure of non heat treated steel can still be easily recognized as being of the step type (Fig. 2).

Table 4 - Oxalic acid test: etch structure of AISI 304 L stainless steel as a function of cold plastic deformation and heat treatment conditions

AISI 304L	SA			SA + 10% ROLLED AT R.T.			SA + 10% ROLLED AT -196°C		
TEMPERATURE / TIME	300 °C	400 °C	500 °C	300 °C	400 °C	500 °C	300 °C	400 °C	500°C
0 h		STEP			STEP			STEP*	
1 h	N.T.	STEP	STEP	N.T.	STEP	STEP	N.T.	STEP*	E.I.G.
10 h		STEP	STEP		STEP	STEP		E.I.G.	E.I.G.
100 h	STEP	STEP	STEP	STEP	STEP	STEP	STEP*	E.I.G.	E.I.G.
1000 h	STEP	STEP	DITCH	STEP	STEP (E.I.G.)	DITCH (E.I.G.)	STEP*	E.I.G.	E.I.G. (DITCH)

SA + 30% ROLLED AT R.T.	SA + 50% ROLLED AT R.T.	SA+ 30% ROLLED AT -196°C	SA + 50% ROLLED AT -196°C
STEP	STEP*	STEP*	STEP*

Notes: N.T. = Not Tested; E.I.G. = Etch Inside the Grain. * = See text.

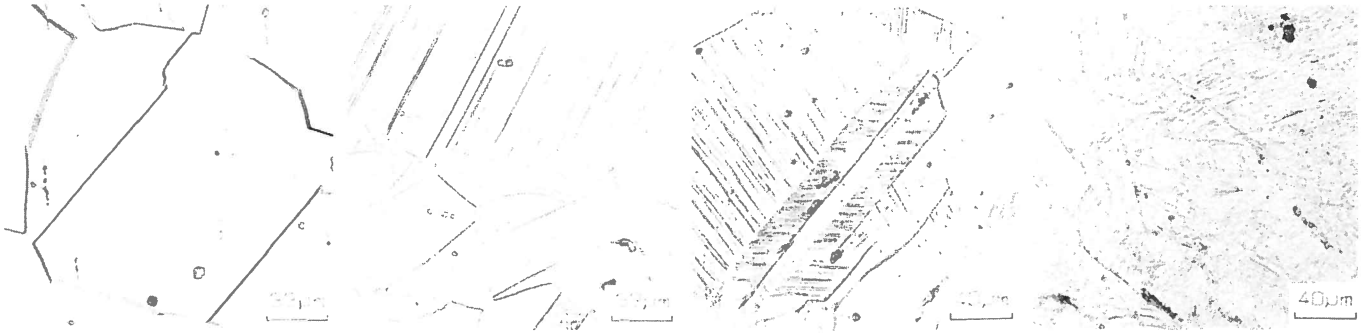

Figure 2- Oxalic acid test: etch structure of AISI 304L stainless steel rolled at R.T. by 0% (a), 10% (b), 30% (c), 50% (d)

Figure 3- Oxalic acid test: etch structure of AISI 304L stainless steel rolled at -196 °C by 10% (a), 30% (b), 50% (c)

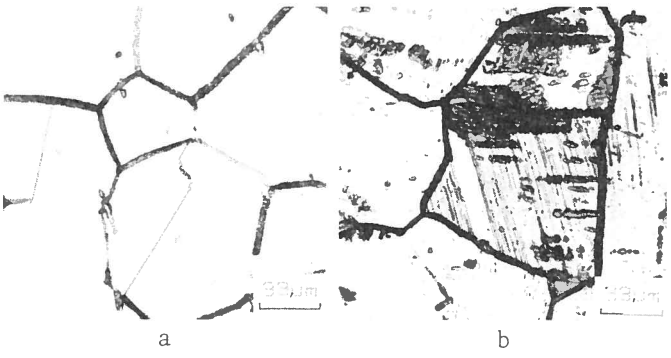

Figure 4 - Oxalic acid test: etch structure of AISI 304L stainless steel: SA (a) and SA + 10% rolled at R.T. (b), after heat treatment at 500 °C for 1000 h

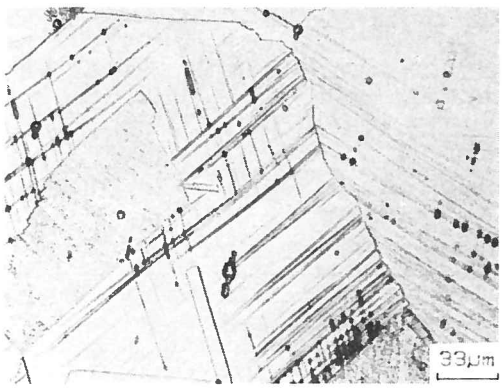

Figure 5 - Oxalic acid test: etch structure of AISI 304L stainless steel SA + 10% rolled at R.T., after heat treatment at 400 °C for 1000 h

The picture changes for the testpieces containing appreciable martensite (50% rolled at R.T. and 10%, 30% and 50% rolled at -196°C); in fact, martensite hinders oxalic acid etching and, where the latter is visible, it induces a different structure from the step structure usually found in austenitic stainless steels (Figs. 2 and 3). However, in these cases too, structure is designated "step" to signify that no specific attack (such as grooves at grain boundary or inside the grain) occurred as a consequence of the heat treatment. For the steel rolled by 10% at -196°C, etching inside the grain after the oxalic acid test already occurs on specimens treated 10 h at 400°C or 1 h at 500°C; grain boundary etching is evident after 1000 h at 500°C (Figs. 3a and 6).

Oxalic acid etching seems to confirm that the deformation bands and any martensite, both induced by cold rolling, accelerate the precipitation of chromium-rich carbides inside the grain. This effect is especially evident in the presence of martensite. For the specific heat treatments performed, precipitation at grain boundary is not so affected as precipitation in-

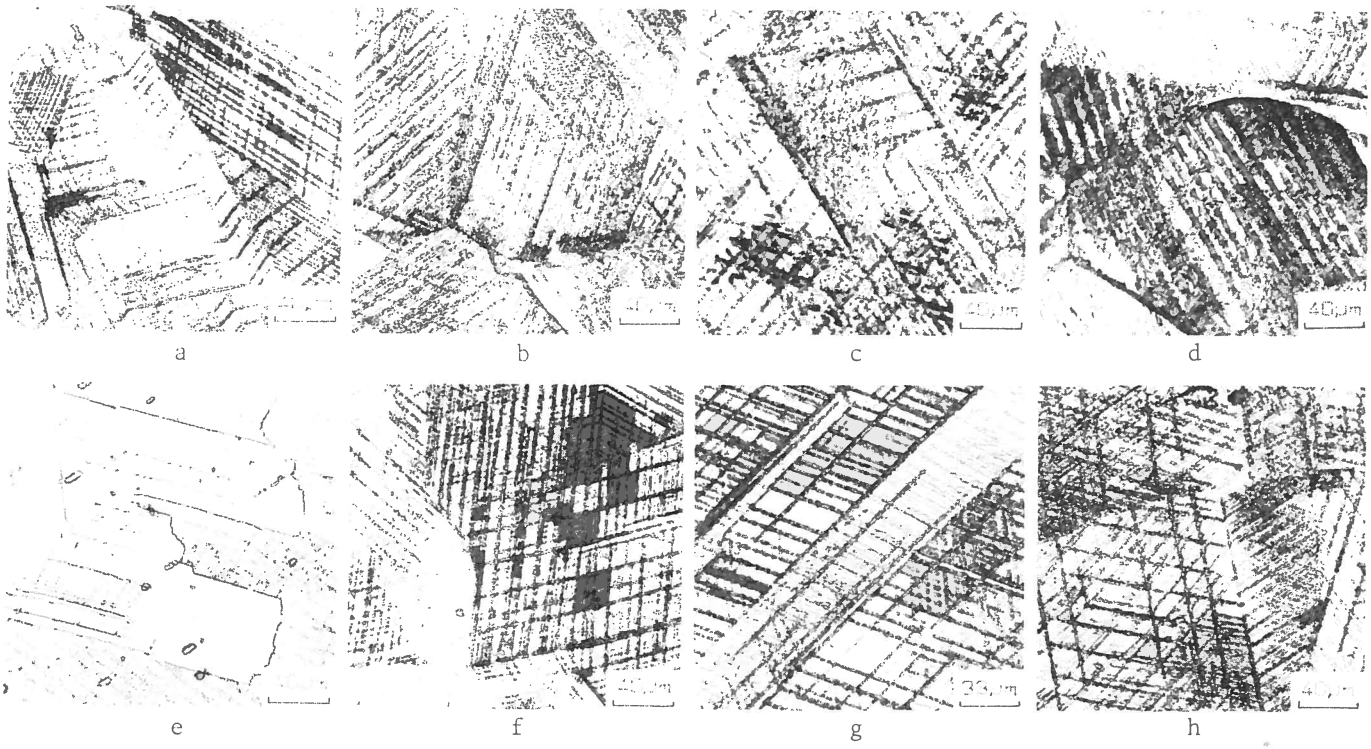

Figure 6- Oxalic acid test: etch structure of AISI 304L stainless steel SA + 10% rolled at -196 °C, after heat treatment at 500 °C for 1 h (a), 10 h (b), 100 h (c), 1000 h (d), or at 400 °C for 1 h (e), 10 h (f), 100 h(g), 1000 h (h)

side grain is. As further confirmation, carbides of the $M_{23}C_6$ type were observed by transmission electron microscopy in an earlier study (10). The carbides were finely distributed within the grain in an AISI 304L steel testpiece, rolled by 50% at -196°C and heat treated at 400°C for 1000 h.

Fig. 7 shows the testpiece weight loss vs time of immersion in the modified Strauss test solution.

In the case of both non-rolled steel and R.T.-10% rolled steel, treated at 500°C for 1000 h, the weight loss is greater than for the other heat treatments (Figs. 7a, b), because of the onset of intergranular etching evidenced under the microscope (Fig. 8). In the case of rolled steel, the weight loss of a testpiece treated at 500°C for 1000 h is greater because of the onset of widespread grain dropping (G.D.) and severe etching inside the grain in correspondence with the deformation bands. This etching does not occur in non-rolled steel and is very slight in the R.T.-10% rolled steel, subjected to the other heat treatments.

The weight loss of steel rolled by 10% at -196°C is significantly higher than those reported before (Fig. 7c). After treating at 500°C the attack is more severe than for an untreated testpiece, as early as after 1 h; the severity increases with the time of heat treatment (however, the weight loss of a testpiece treated at 500°C for 1 h only slightly deviates from that of an SA testpiece). At 400°C, significant weight losses occur only after 100 h and 1000 h; such losses are however greater than those for the corresponding 500°C treatments. The weight loss of testpieces treated at 300°C equals that of an SA testpiece. The attack in steel rolled by 10% at -196°C essentially occurs inside the grain; for a testpiece treated at 500°C for 1000 h only, it also occurs on grain boundary (Fig. 9a). The testpieces where dropping of parts of grain (P.G.D.) takes place (Fig. 9b) exhibit the greatest weight loss, while in the cases examined before (non-rolled or R.T.-10% rolled steel) dropping always affects the whole grain.

In the light of the results of conventional tests and from the chromium-depletion theory, the following can be reasonably assumed.

1. The presence of deformation bands and chiefly of martensite accelerates the precipitation of chromium-rich carbides, as it increases the number of nucleation sites and assists diffusion processes in the matrix. Consequently, carbides precipitate inside the grain.

2. In the carbide-adjacent zone a chromium-depleted, easily attacked area forms in a very short time because of the rather low temperature. These areas are therefore arranged according to the carbide precipitation morphology, i.e., that of the deformation bands and possible martensite laths.

3. Whenever these chromium-depleted areas are sufficiently extended (sensitized steel) and, more important, continuous, etching penetrates in depth during the modified Strauss test causing partial or total grain dropping as in rolled material. In case of a more limited precipitation, the chromium-depleted patches are smaller and isolated and the weight loss during the

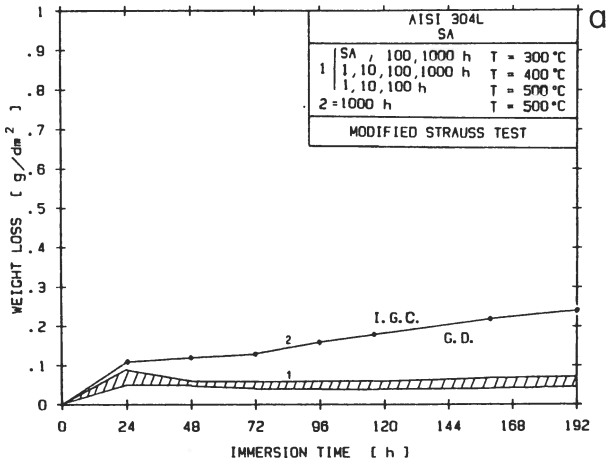

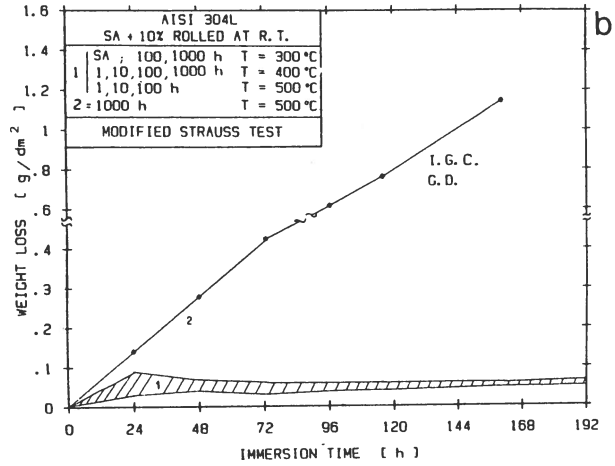

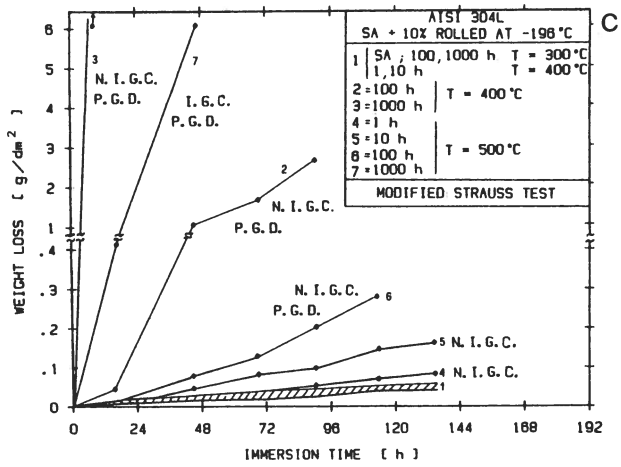

Figure 7 - Modified Strauss test: weight loss of AISI 304L stainless steel as a function of immersion time and of cold plastic deformation and heat treatment conditions

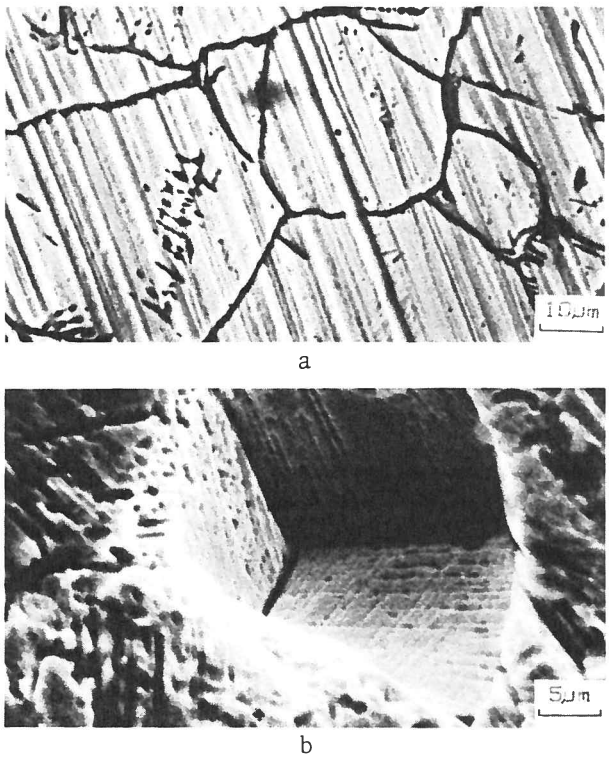

Figure 8 - Modified Strauss test: SEM photographs of AISI 304L stainless steel: SA (a) and SA + 10% rolled at R.T. (b), after heat treatment at 500 °C for 1000 h

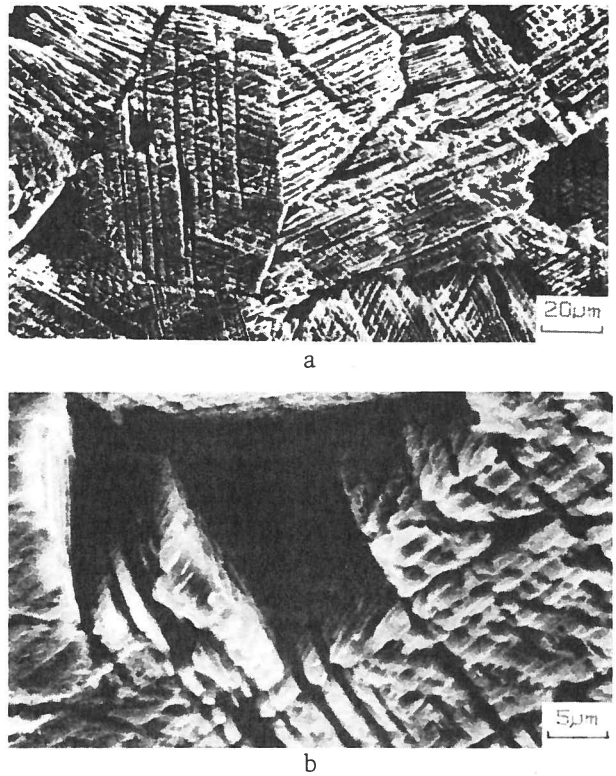

Figure 9 - Modified Strauss test: SEM photographs of AISI 304L stainless steel SA + 10% rolled at -196 °C, after heat treatment at 500 °C for 1000 h

modified Strauss test does not bring out the degree of steel sensitization which is generally quite slight and insufficient to cause a significant attack in the usual environments. However, even such a low sensitizing may be unacceptable in the presence of tensile stress and in a specific environment (I.G.S.C.C.); hence the need for other methods such as EPR (11-13), which was also adopted here to study its validity for cold-rolled materials.

The morphology of the etching inside the grain during the modified Strauss test on rolled steel does not depend on the sensitization treatment and is essentially the same for both solution-annealed and sensitized material; what changes is etching severity. In fact, the solution-annealed and rolled material is not uniformly etched, and the etch pattern is affected by the presence of deformation bands and martensite - the same factors affecting carbide precipitation - and by the etching potential (14).

The EPR test results (Fig. 10 and Table 5) substantially confirm those of the conventional tests on non-rolled steel or on steel rolled by 10% at -196°C. If we assume, with Clarke, that the material sensitization threshold of the normalized charge P_a = Q/GBA is 2C/cm^2 (to which the value L of the specific charge Q/A of Fig. 10 corresponds, A being the specimen surface area), we note that:

- for non-rolled steel, sensitization occurs on the testpiece treated at 500°C for 1000 h (Fig. 10a);
- for steel rolled by 10% at -196°C, sensitization occurs on all testpieces treated at 500°C and of those treated at 400°C, only on that treated for 1000 h (Fig. 10c).

The attack of Fig. 11b occurs however for an average value of P_a = 0.845 C/cm^2 (or for Q/A = 12.66 mC/cm^2) exhibited by steel rolled by 10% at -196°C after treating at 400°C for 100 h. The Fig. 11a also shows for comparison purposes, the aspect of the steel after heat trea-

Table 5 - EPR test: specific anodic charge Q/A (mC/cm^2) for AISI 304L stainless steel as a function of cold plastic deformation and heat treatment conditions

AISI 304L	SA			SA + 10% ROLLED AT R.T.			SA + 10% ROLLED AT -196 °C		
TEMPERATURE / TIME	300 °C	400 °C	500 °C	300 °C	400 °C	500 °C	300 °C	400 °C	500 °C
0 h		0.28 <u>0.61</u> 0.94 (0.027)			59.20 0.64 57.48 101 7.17 <u>45.13</u> (3.329)			1.82 2.02 <u>1.92</u> -	
1 h		1.74 3.00 1.91 2.78 <u>1.83</u> <u>2.89</u> (0.082) (0.130)			13.06 22.48 <u>24.94</u> (1.840)	13.61 4.09 8.51 3.31 156 39.13 179 5.17 <u>51.15</u> (3.773)		1.06 822 1.20 675 <u>1.73</u> <u>749</u> - -	
	N.T.			N.T.			N.T.		
10 h		0.65 6.26 0.97 2.30 <u>0.81</u> <u>4.63</u> (0.036) (0.209)			16.25 1.84 44.17 <u>20.75</u> (1.531)	194.18 58.27 358.93 247.10 <u>214.62</u> (15.83)		1.75 1898 2.23 1854 <u>1.99</u> <u>1876</u> - -	
100 h	4.75 2.55 <u>3.65</u> (0.164)	0.73 18.21 0.87 17.71 <u>0.80</u> <u>17.96</u> (0.036) (0.809)		94.96 62.08 <u>78.52</u> (5.793)	17.19 12.74 1.63 108.01 <u>34.89</u> (2.574)	205.19 168.13 207.51 <u>193.61</u> (14.28)	2.22 3.20 3.27 <u>2.90</u> -	16.18 2018 9.13 2454 <u>12.66</u> <u>2236</u> - -	
1000 h	2.17 3.28 <u>2.73</u> (0.123)	3.92 118.7 1.15 137.2 0.88 1.36 <u>127.9</u> <u>1.83</u> (0.082)		2.30 3.56 1.30 <u>2.39</u> (0.176)	9.78 18.58 12.34 <u>13.57</u> (1.001)	639 597 <u>618</u> (45.62)	1.43 1.06 1.05 1.09 <u>1.16</u> -	539 3590 657 3549 <u>598</u> <u>3570</u> - -	

Notes: the underlined numbers give the average of the listed Q/A values; the numbers between brackets give the (average) normalized charge P_a = Q/GBA (C/cm^2).

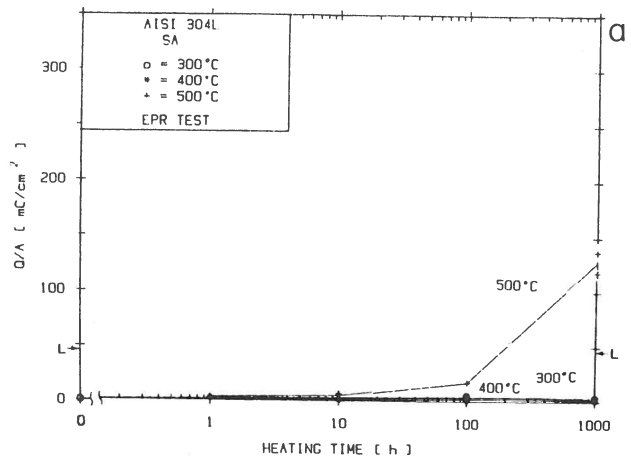

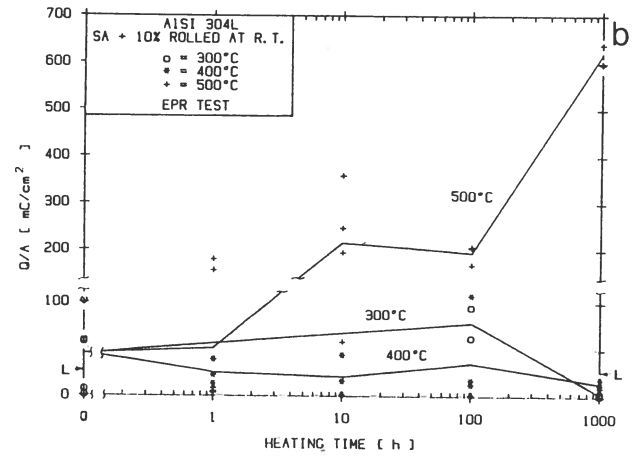

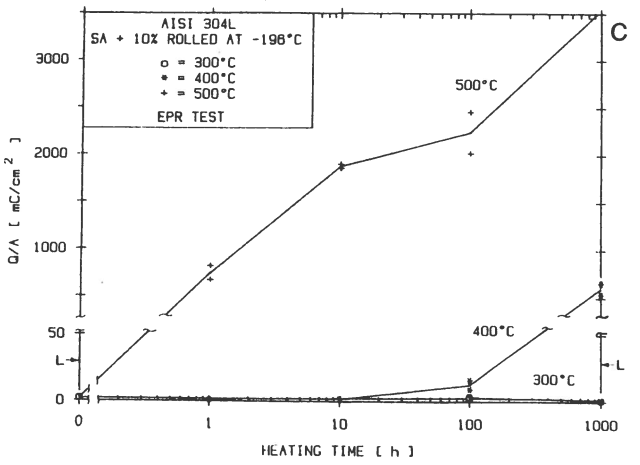

Figure 10- EPR test: specific anodic charge for AISI 304L stainless steel as a function of cold plastic deformation and heat treatment conditions. L = Clarke's value for sensitization

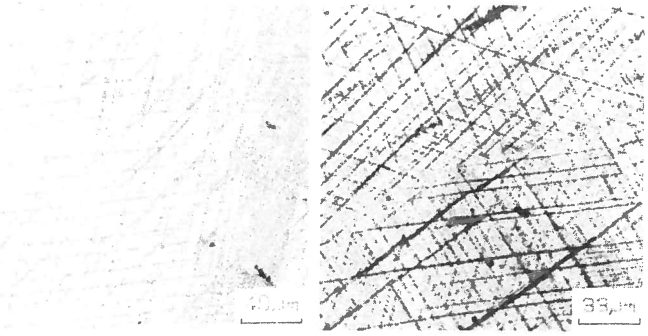

Figure 11- EPR test: etch structure of AISI 304L stainless steel SA + 10% rolled at -196 °C, after heat treatment at 400 °C for 10 h (a) and 100 h (b)

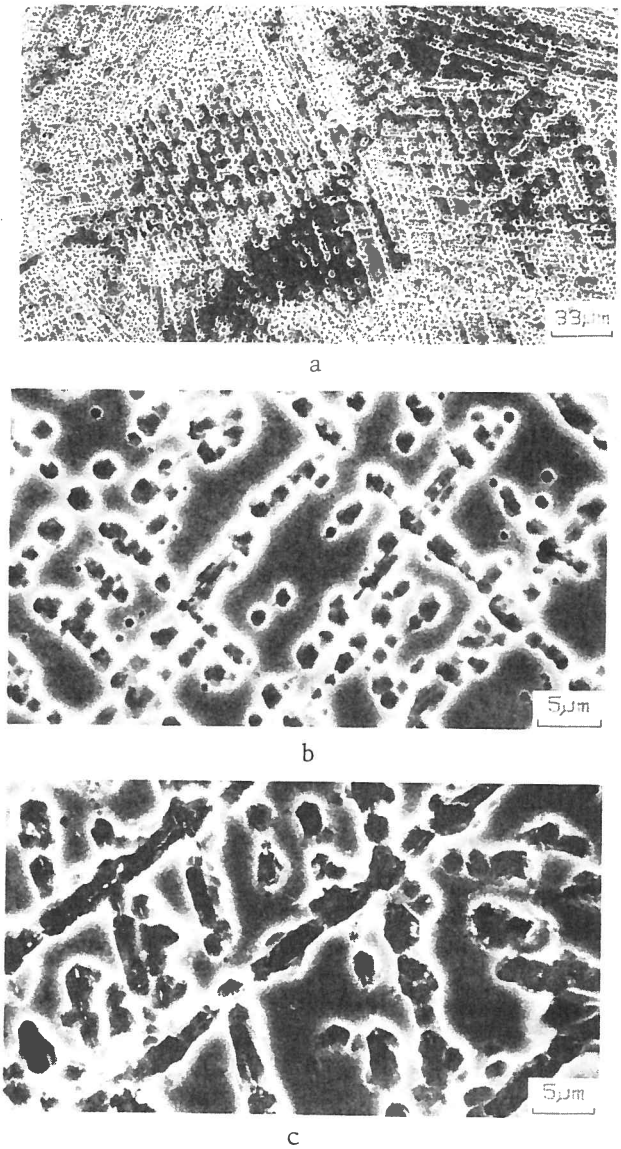

Figure 12- EPR test: SEM photographs of AISI 304L stainless steel SA + 10% rolled at -196 °C, after heat treatment at 400 °C for 1000 h (a), or at 500 °C for 10 h (b) and 1000 h (c)

ting for 10 h only. As for conventional tests, intergranular attack occurs after the EPR test only on those testpieces treated at 500°C for 1000 h. No localized attack is evident on testpieces of non- rolled steel submitted to other heat treatments, while for steel rolled at -196°C, etching inside the grain, as previously found by conventional tests, is always present. This etching is especially deep on sensitized testpieces (Fig. 12). Because of the etch morphology, normalizing the circulating charge with respect to grain boundary area is no longer justifiable for steel rolled by 10% at -196°C, nor is the limit value of 2 C/cm^2 for P_a valid.

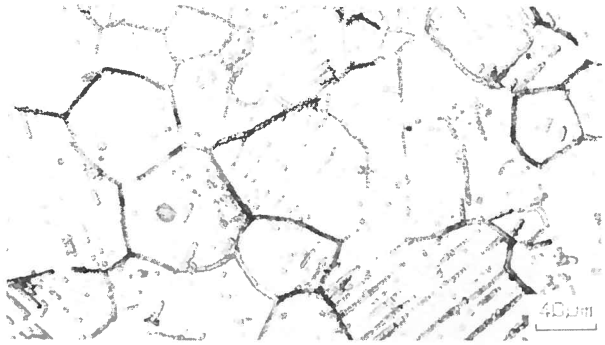

a

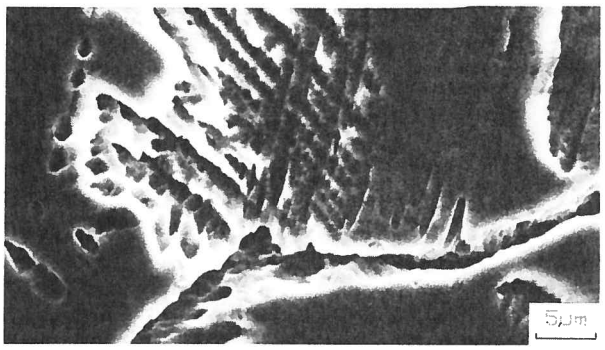

b

Figure 13- EPR test: Micrograph (a) and SEM photograph (b) of AISI 304L stainless steel SA + 10% rolled at R.T., after heat treatment at 500 °C for 1000 h

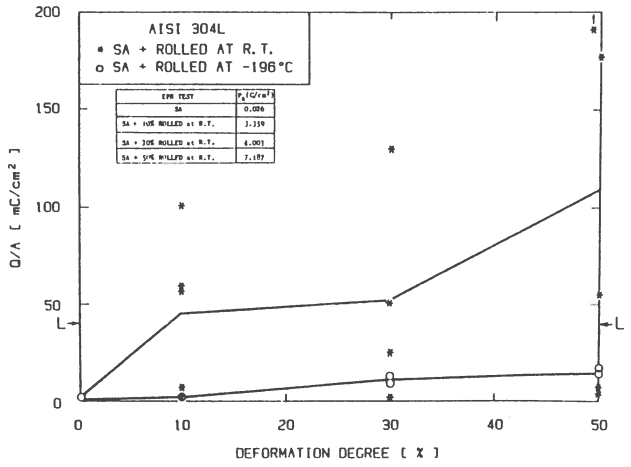

Figure 14- EPR test: specific anodic charge for AISI 304L stainless steel as a function of cold plastic deformation conditions

For steel rolled by 10% at room temperature the EPR test results are widely scattered as compared to the other cases (Fig. 10b and Table 5), and both P_a and Q/A are high even under SA conditions. Intergranular etching is apparent only on the testpiece treated at 500°C for 1000 h (Fig. 13). It is thus clear that the degree of sensitization of a steel rolled by 10% at room temperature cannot be determined by the EPR test. This is probably due to the formation, in the presence of rolling-induced residual stresses, of a more flawed passivating film which is more prone to attack when potential is running through activity range during the EPR test. In fact, Fig. 14 shows reactivation to increase and to have correspondingly more scattered values when the degree of deformation of a solution annealed, R.T. rolled material increases. A comparison of Figs. 14 and 1 further shows this effect to be due to the deformation of the austenitic matrix, since martensite reduces and stabilizes reactivation. However, the specific charge Q/A circulated when EPR-testing the solution annealed, rolled pieces slightly increases with the martensite content, according to a linear law (Q/A [mC/cm^2] $\simeq$ 0.17 martensite [%]).

The temperature-time sensitization (TTS) curves obtained by the modified Strauss and EPR tests, are given in Fig. 15. The sensitization range of a non-rolled steel, determined by the modified Strauss test, coincides with that obtained by the EPR test, although the latter can also evidence shorter 500°C treatments. This also holds true for steel rolled by 10% at -196°C, when 12.5 mC/cm^2 is assumed as the threshold value for Q/A. The sensitization range for 500°C treatments is broader when measured by EPR and coincides with that deduced from the oxalic acid etch test (Table 4). For treatments at 400°C, the weight loss test appears to be more sensitive than the EPR test (probably in the former dropping of parts of grain occurs more easily).

CONCLUSIONS

1. Cold rolling by 10% accelerates steel sensization at temperatures ranging from 500 to 300°C. The effect is more pronounced when α'-martensite is formed.

2. The etching morphology varies for rolled and sensitized testpieces: etching occurs also or exclusively inside the grain.

3. The EPR test for non-rolled AISI 304L steel shows good correlation with the modified Strauss test; specifically, the sensitization threshold value of the normalized charge P_a = Q/GBA = 2 C/cm^2 is confirmed.

4. The EPR test on steel rolled by 10% at -196°C (high martensite-content) can also be correlated to the modified Strauss test. In this case, the circulated charge should not be normalized with respect to grain boundary area, since attack mostly occurs inside the grain in correspondence with the martensite or deformation bands, in areas the extension of which only depends on the deformation degree. Microstructural examinations

and a comparison with the weight loss measurements during the modified Strauss test show the threshold value of the circulated charge during the EPR tests to be Q/A = 12.5 mC/cm^2. This value should indicate sensitization in materials having undergone a thermo-mechanical treatment similar to that of AISI 304L rolled by 10% at -196°C (martensite content ≃ 26%), but it was not obtained by results that could be directly correlated with the actual corrosion behaviour of the steel.

5. The sensitivity of the weight loss measurement during the modified Strauss test on materials rolled at -196°C appears to be greater than that of the same test on non-rolled material, because of possible dropping of parts of grain.

6. The EPR test is significantly affected by any residual stresses induced by R.T. rolling (in the absence of α'-martensite), and is therefore unapplicable in practice starting from rolling ratios as low as 10% (i.e., for deformation degrees that are rather close to those induced in the steel during fabrication). This result should be carefully considered also in view of a draft standard for the EPR test, and the effect of deformation degrees ranging from 0 to 10% on this test should be investigated.

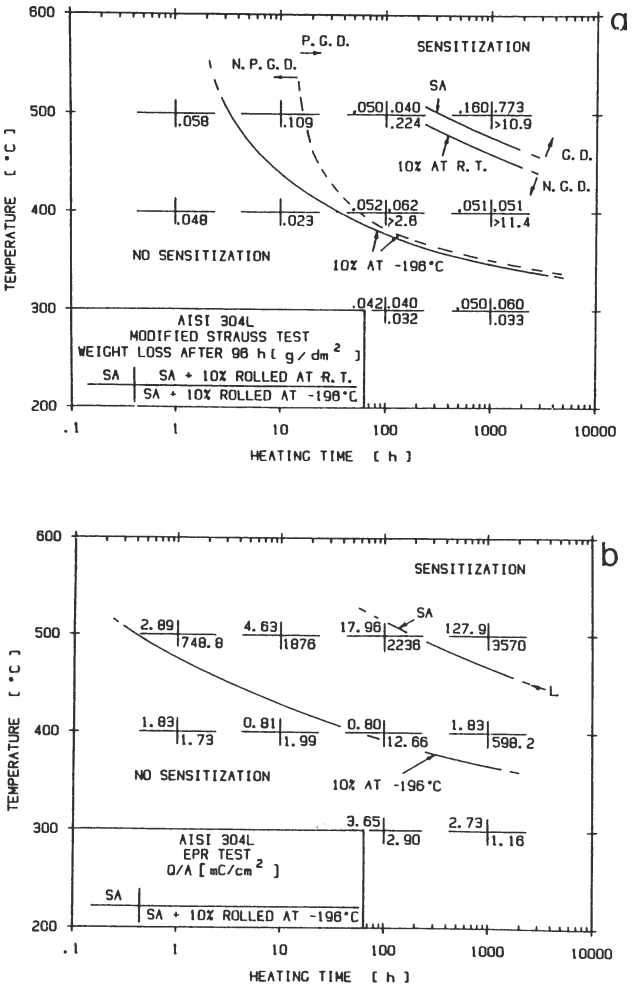

Figure 15- Modified Strauss test (a) and EPR test (b): TTS curves for AISI 304L stainless steel as a function of cold plastic deformation conditions

---

We would like to give our tribute to Professor Dany Sinigaglia, a dear friend and distinguished scientist, who helped us initiate this research but passed away before his time on July 10th, 1983.

REFERENCES

1. Pipe Crack Study Group, U.S. Nuclear Regulatory Commission NUREG 0531, 1979.

2. Briant, C.L., and A.M. Ritter, Metall. Trans. 11A, 2009 (1980).

3. Briant, C.L., Corrosion 38, 596 (1982).

4. Pednekar, S., and S. Smialowska, Corrosion 36, 565 (1980).

5. Solomon, H.D., Corrosion 36, 356 (1980).

6. Solomon, H.D., and C.D. Lord, Corrosion 36, 395 (1980).

7. Tedmon, C.S., et al., Corrosion 27, 104 (1971).

8. Mazza, B., et al., J. Electrochem. Soc. 123, 1157 (1976).

9. Mazza, B., et al., J. Electrochem. Soc. 126, 2075 (1979).

10. Cigada, A., et al., Corrosion Sci. 22, 559 (1982).

11. Clarke, W.L., et al., General Electric Report GEAP-21382, 1976; Intergranular corrosion of stainless alloys, ASTM-STP 656, p. 99, 1978.

12. Sinigaglia, D., et al., La Metallurgia Italiana 74, 367 (1982) (English transl.).

13. Sinigaglia, D., et al., La Metallurgia Italiana 75, 473 (1983) (English transl.).

14. Salvago, G., et al., Corrosion Sci. 23, 507 (1983); ibidem 23, 515 (1983); ibidem 23, 1073 (1983).